Instantaneous charge and dielectric response to terahertz pulse excitation in TTF-CA

Hiroki Gomi, Naoto Yamagishi, Tomohito Mase, Takeshi J. Inagaki, and Akira Takahashi

Phys. Rev. B **95**, 094116 — Published 20 March 2017

DOI: 10.1103/PhysRevB.95.094116

Instantaneous charge and dielectric response to THz pulse in TTF-CA

Hiroki Gomi[1], Naoto Yamagishi[1], Tomohito Mase[1], Takeshi J. Inagaki[2], and Akira Takahashi[1]

[1] *Department of Physical Science and Engineering, Nagoya Institute of Technology, Gokiso-Cho, Showa-ku, Nagoya 466-8555, Japan and*

[2] *Graduate School of Materials Science, Nara Institute of Science and Technology, Ikoma, 630-0192, Japan*

(Dated: February 22, 2017)

Abstract

We present the results of exact numerical calculations of the dielectric properties of tetrathiafulvalene-p-chloranil (TTF-CA) using the extended Hubbard model. The electronic polarization $\bar{P}_{\rm el}$ of the ionic ground state is obtained by directly calculating the adiabatic flow of current. The direction of $\bar{P}_{\rm el}$ is opposite to polarization $\bar{P}_{\rm ion}$ owing to ionic displacement, and $|\bar{P}_{\rm el}|$ is much larger than $|\bar{P}_{\rm ion}|$, showing that in the ionic phase, TTF-CA is an electric ferroelectric. Furthermore, we numerically calculate the dynamics induced by THz pulse excitation. In the ionic phase, there exists an almost exact linear relationship between $\Delta\rho(t)$ and $E(t)$, and between $\Delta P_{\rm el}(t)$ and $E(t)$ in the realistic range of the excitation magnitude, where $\Delta\rho(t)$ ($\Delta P_{\rm el}(t)$) is the charge transfer (electric polarization) variation induced by the THz pulse, and $E(t)$ is the electric field of the pulse at time t. The absolute value of $\Delta\rho(t)$ is much smaller in the neutral phase than that in the ionic phase. These results are consistent with those of experiments, and originate from the adiabatic nature of the THz pulse excited state.

PACS numbers: 77.80.-e, 82.53.Xa, 73.20.Mf, 78.30.Jw

I. INTRODUCTION

Ferroelectric materials are widely used in various devices such as a random access memory, capacitors, sensors, piezoelectric actuators, and optical devices.[1–3] In conventional ferroelectrics, electric polarization is governed by the rotation of polar molecules (order-disorder-type) or displacement of ions (displacive-type). Recently, ferroelectricity that arises from electron transfer has been observed in some materials. This new type of ferroelectricity is termed electronic ferroelectricity.[4,5] Multiferroicity,[6–12] where the ferroelectricity is driven by spin ordering, and charge-order-driven ferroelectricity,[13–19] where electric polarization is caused by an electronic charge order without inversion symmetry, are representative examples of electronic ferroelectricity. If their ferroelectric polarization could be controlled in the picosecond time domain, ferroelectric materials could be used for advanced switching devices. The typical time constants of polarization change for conventional ferroelectric materials vary from microseconds to milliseconds, but much faster polarization switching is expected for electronic ferroelectricity.

TTF-CA is an organic charge-transfer compound composed of an alternately stacked donor (D), tetrathiafulvalene (TTF), and acceptor (A), p-chloranil (CA).[20] TTF-CA exhibits a neutral to ionic phase transition at $T_{\rm c} \simeq 81$ K.[20–26] The electronic structure of these two phases is schematically shown in Fig. 1. In the ionic phase, an electron is transferred from D to A, and the phase is stable when the electrostatic energy gain overcomes the energy cost of molecular ionization. Because of orbital hybridization between D and A, the charge transfer $\bar{\rho}$ from A to D is not 1 (0), and $\bar{\rho} \sim 0.6$ ($\bar{\rho} \sim 0.3$) in the ionic (neutral) phase.[27,28] Dimerization occurs in the ionic phase.[29–31] Pairs of D and A connected by shorter bonds are indicated by the oval in Fig. 1.

Previously, TTF-CA in the ionic phase had been regarded as a displacive-type ferroelectric, the polarization of which results from the displacement of static point charges of ions.[32,33] However, recent experimental $P-E$ measurements[34] and theoretical studies[35–38] have revealed that the direction of the net polarization is opposite to the ionic displacement, and the absolute value of net polarization is much larger than that due to the ionic displacement. This shows that ionic phase TTF-CA is an electronic ferroelectric, the polarization of which mainly originates from charge transfer between D and A.

Recently, Miyamoto *et al.* carried out THz-pump optical-probe and SHG-probe measure-

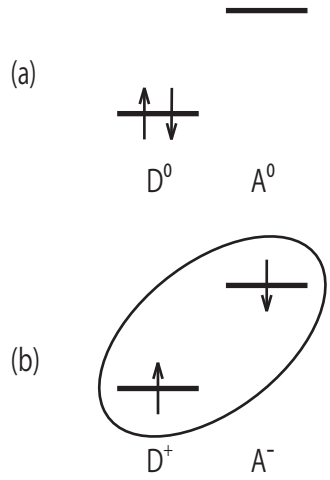

FIG. 1: Schematic representation of the electronic structures of the (a) neutral and (b) ionic phases of TTF-CA. The horizontal lines show the highest occupied molecular orbital of D and the lowest unoccupied molecular orbital of A, and the arrows represent the electron spins. Neutral (ionic) D and A are denoted by D^0 and A^0 (D^+ and A^-), respectively.

ments on TTF-CA, and showed a linear relationship between $\Delta\rho(t)$ and $E(t)$ and between $\Delta P_{\rm el}(t)$ and $E(t)$, where $\Delta\rho(t)$ ($\Delta P_{\rm el}(t)$) is the charge transfer (electronic polarization) variation induced by the THz pulse, and $E(t)$ is the electric field waveform of the THz pulse at time t.[39] This result indicates that the polarization amplitude can be modulated on the picosecond time scale with a THz pulse. This opens up the possibility of the application of this material to optical switching.

However, the origin of the instantaneous response has not been clarified yet. Therefore, in this work, we theoretically investigate the dynamics induced by THz pulse excitation from numerical calculations in the extended-Hubbard model for TTF-CA. There have been several works on the THz pulse induced dynamics in the Hubbard-like model for one-dimensional Mott insulators.[40,41] The THz pulse induced dynamics is essentially different from that induced by a light pulse, and interesting results such as doublon-hole pair production, and switching of Coulomb interaction from repulsive to attractive, have been obtained. It is found in the present work that the experimental results are reproduced well by the numerical calculations, and the adiabatic response is the origin of the instantaneous charge and dielectric response of TTF-CA to a THz pulse.

II. MODEL

We adopt the extended Hubbard Hamiltonian for TTF-CA coupled with the electric field of a THz pulse. We consider a half-filled periodic 1D chain with system size N =14. We first introduce the following set of binary electron operators:

$$\hat{\rho}^{\sigma}_{n,m} = c^{\dagger}_{m,\sigma} c_{n,\sigma} \tag{1}$$

where $c^{\dagger}_{n,\sigma}$ ($c_{n,\sigma}$) creates (annihilates) an electron of spin σ at site n. Using this notation, the Hamiltonian is given by

$$\begin{aligned} H(t) \;=\; & \sum_{n=1,\sigma}^{N} \alpha'(-1)^n \hat{\rho}^{\sigma}_{n,n} + \sum_{n=1,\sigma}^{N} (\bar{\beta} + (-1)^n \beta')(\hat{\rho}^{\sigma}_{n+1,n} e^{i\bar{A}(t)} + \hat{\rho}^{\sigma}_{n,n+1} e^{-i\bar{A}(t)}) \\ & + \; U \sum_{n} \hat{\rho}^{\uparrow}_{n,n} \hat{\rho}^{\downarrow}_{n,n} + V \sum_{n,\sigma,\sigma'} \hat{\rho}^{\sigma}_{n,n} \hat{\rho}^{\sigma'}_{n+1,n+1}, \end{aligned} \tag{2}$$

where D (A) is placed at the odd–numbered (even–numbered) sites. We adopt standard notation for the Coulomb integral and the transfer integral in quantum chemistry.[42] The first term describes the site energy, where $2\alpha'$ shows the difference in orbital energy between the highest occupied molecular orbital of D and the lowest unoccupied molecular orbital of A. The second term describes the transfer of electrons, and the electron–light coupling is introduced as the Peierls phase into the transfer integrals, where $\bar{\beta}-\beta'$ ($\bar{\beta}+\beta'$) is the transfer integrals for a shorter (longer) bond when $\bar{A}(t)$, the dimensionless vector potential at time t, is 0. A shorter (longer) bond is placed at the odd–numbered (even–numbered) bond, and $|\beta'|$ shows the magnitude of bond length alternation. The third and the fourth terms describe the on-site Coulomb interaction and the Coulomb interaction between neighboring sites, respectively, where U is the on-site Coulomb interaction energy and V is the Coulomb interaction energy between neighboring sites. The electric Hamiltonian $H_{\rm e}$ is given by $H(t)$ for $\bar{A}(t) = 0$, and the ground state of $H_{\rm e}$ is denoted by $|\phi_0\rangle$. We numerically calculate $|\phi_0\rangle$ using the Lanczos method.

We consider the dimensionless vector potential $\bar{A}(t)$ of a half-cycle pulse given by

$$\bar{A}(t) = \frac{\bar{A}}{2}\{1 + \tanh(\frac{t}{D})\}, \tag{3}$$

where $\bar{A}$ is the amplitude, and D is the duration time. The vector potential $A(t)$ is given by $A(t) = \bar{A}(t)/(ea)$, where e is the elementary charge, and $a = 3.6$ Å[29] is the average lattice spacing along the one-dimensional direction. We numerically solve the time-dependent

Schrödinger equation subject to the pulse with the initial condition $|\psi(-\infty)\rangle = |\phi_0\rangle$, where $|\psi(t)\rangle$ is the solution at time t.

The elements of the single density matrix for $|\psi(t)\rangle$ are denoted by $\rho^{\sigma}_{n,m}(t) = \langle\psi(t)|\hat{\rho}^{\sigma}_{n,m}|\psi(t)\rangle$, while those for $|\phi_0\rangle$ are denoted by $\bar{\rho}^{\sigma}_{n,m} = \langle\phi_0|\hat{\rho}^{\sigma}_{n,m}|\phi_0\rangle$. The expectation values of the considered physical quantities are given by these.

Because all the even-numbered (odd-numbered) sites are equivalent, the charge distribution of $|\psi(t)\rangle$ ($|\phi_0\rangle$) can be described by the charge transfer $\rho(t)$ ($\bar{\rho}$) from D to A, where $\rho(t) = \sum_{\sigma}\rho^{\sigma}_{2,2}(t)$ and $\bar{\rho} = \sum_{\sigma}\bar{\rho}^{\sigma}_{2,2}$. In the ionic (neutral) phase, $\bar{\rho}$ is nearly equal to one (zero). The charge transfer $\rho(t)$ can be decomposed into two parts as

$$\rho(t) = \bar{\rho} + \Delta\rho(t), \tag{4}$$

where $\Delta\rho(t)$ is the charge transfer variation induced by the THz pulse.

III. RESULTS

We first determine the parameters for the neutral phase and the ionic phase. Because bond length alternation does not occur, $\beta' = 0$ holds in the neutral phase. It has been shown that the light absorption spectrum of the neutral phase can be reproduced well with the following parameters: $\bar{\beta} = -0.17$, $\alpha' = 0.15$, $U = 2.41$, and $V = 1.07$.[43] Here and hereafter, we use eV as the unit of energy. The above values of $\bar{\beta}$, U and V are adopted for both the neutral and ionic phases. To determine α' and β', we calculate the dependence of the light absorption spectrum $\alpha(\omega)$, $\bar{\rho}$, and $\Delta\rho(t)$ on them.

The α' dependence of $\bar{\rho}$ for $\beta' = 0$ and 0.02 is shown in Fig. 2. In the small (large) α' region, $\bar{\rho} \simeq 1$ ($\bar{\rho} \simeq 0.1$) holds, and the ground state is an ionic (a neutral) state. In the phase boundary region between these two regions, $\bar{\rho}$ decreases rapidly with increasing α'.

The values of α' that reproduce the experimentally observed values $\bar{\rho} = 0.3$ and $\bar{\rho} = 0.6$ for the neutral and ionic phases, respectively,[27,28] are both in the phase boundary region. However, because $|\Delta\rho(t)|$ is much larger than the experimentally estimated value in the phase boundary region as will be shown later, we adopt α' outside this region.

In the ionic phase, we adopt the parameters $\alpha' = 0.13$ and $\beta' = 0.02$. These values reproduce $\alpha(\omega)$ and $\Delta\rho(t)$ reasonably, but give $\bar{\rho} = 0.93$, which is significantly larger than that experimentally observed. Furthermore, the ratio $|\beta'/\bar{\beta}| = 0.14$ is consistent with the

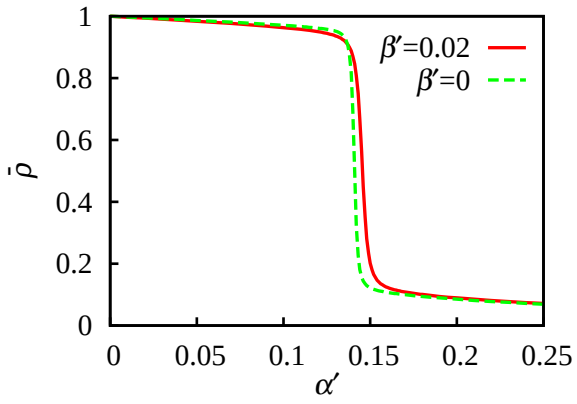

FIG. 2: (Color online) The α' dependence of $\bar{\rho}$ for $\beta' = 0$ and $\beta' = 0.02$.

difference between the length of the longer and shorter bonds.[29] A much larger ratio ($|\beta'/\bar{\beta}| \simeq 0.5$) is proposed from numerical calculations of the electron-lattice couple system.[44] However, such large $|\beta'|$ results in $\alpha(\omega)$ being greatly different from that observed experimentally.

In the neutral phase, we adopt $\alpha' = 0.158$ and $\beta' = 0$, which reproduce $\alpha(\omega)$ well. These values give $\bar{\rho} = 0.11$, which is significantly smaller than the experimentally observed value. These parameters are consistent with previous theoretical works.[26,35,45–49]

A. electric polarization of the ionic phase ground state

In this section, we calculate the electronic polarization per unit cell $\bar{P}_{\rm el}$ of the ionic ground state. It should be emphasized that $\bar{P}_{\rm el}$ cannot be determined from the charge distribution in the unit cell, but it can be determined from the adiabatic flow of current.[50–53] The current can be calculated from the Berry phase in models based on density functional theory,[50,54] and other methods have been proposed.[55,56] In this paper, it is directly calculated from the current for the many-body wave function to fully take the strong correlation effect into account. The current operator $\hat{i}_n$ for bond n, which connects sites n and $n+1$, is given by

$$\hat{i}_n(t) = -ie\sum_{\sigma}(\bar{\beta} + \beta'(-1)^n)(\hat{\rho}^{\sigma}_{n+1,n}e^{i\bar{A}(t)} - \hat{\rho}^{\sigma}_{n,n+1}e^{-i\bar{A}(t)}). \tag{5}$$

The expectation values $i_n(t) = \langle\psi(t)|\hat{i}_n(t)|\psi(t)\rangle$ satisfy the equation of charge conservation

$$\frac{\partial}{\partial t}\{e\sum_{\sigma}\rho^{\sigma}_{n,n}(t)\} = i_n(t) - i_{n-1}(t). \tag{6}$$

We introduce an adiabatic parameter λ that scales the electronic parameters leading from the neutral ground state ($\lambda = 0$) to the ionic ground state ($\lambda = 1$). We consider the electronic Hamiltonian $H_{\rm e}(\lambda)$ with the scaled parameters, where $\alpha' = 0.158(1-\lambda) + 0.13\lambda$ and $\beta' = 0.02\lambda$. The ground state of $H_{\rm e}(\lambda)$ is denoted by $|\Phi_0(\lambda)\rangle$. Namely, $|\Phi_0(1)\rangle$ ($|\Phi_0(0)\rangle$) is the ground state of the ionic (neutral) phase. We adiabatically change $\lambda(t)$ from zero to 1 with large time interval T by assuming the relation $\lambda(t) = t/T$, and solve the time-dependent Schrödinger equation

$$i\frac{\partial}{\partial t}|\Psi(t)\rangle = H_{\rm e}(\lambda(t))|\Psi(t)\rangle, \tag{7}$$

with the initial condition $|\Psi(0)\rangle = |\Phi_0(0)\rangle$. Because $H_{\rm e}(0)$ has inversion symmetry, the electronic polarization is zero for the neutral ground state $|\Phi_0(0)\rangle$. Therefore, the electronic polarization $\bar{P}_{\rm el}$ of the ionic ground state $|\Phi_0(1)\rangle$ is given by the time integration of adiabatic current flow as

$$\bar{P}_{\rm el} = \int_0^T dta\langle\Psi(t)|(\hat{i}_{2n-1} + \hat{i}_{2n})|\Psi(t)\rangle, \tag{8}$$

where $\hat{i}_n$ is $\hat{i}_n(t)$ when $\bar{A}(t) = 0$. In Eq. (8), we assume that the bond length of all bonds is equal to a for simplicity. The difference in length between odd–numbered and even–numbered bonds is a few percent of a, so this simplification will affect the present result only slightly.

As T is increased up to 8000 eV^{-1}, $\bar{P}_{\rm el}/(ea)$ converges to -0.802 within an error of 1%. The polarization direction and $|\bar{P}_{\rm el}|$ are consistent with the experimental results (-0.6)[34] and previous theoretical results based on density functional theory. Furthermore, $|\bar{P}_{\rm el}| \gg |\bar{P}_{\rm ion}|$ holds, where $\bar{P}_{\rm ion}$ is the polarization per unit cell arising from the ionic displacement. The present result also shows that electronic polarization is dominant in TTF-CA in the ionic phase.

B. THz pulse induced dynamics in the ionic phase

In this section we show the time variation of $\Delta\rho(t)$ and $\Delta P_{\rm el}(t)$ induced in the ionic phase of TTF-CA by a THz pulse. The electric field of the pulse is given by

$$E(t) = -\frac{1}{2eaD}\bar{A}\cosh^{-2}(\frac{t}{D}). \tag{9}$$

We adopt the duration time $D = 300$ eV^{-1} (201 fs), which is about the same as that used in the experiments, and $1/(2eaD) = 46$ kV/cm. The dependence of the results on D will be discussed later.

We first show how an artifact caused by the finite-size effect can be removed from the numerical results. As will be shown later, the adiabatic approximation holds well for the solution $|\psi(t)\rangle$ of the time-dependent Schrödinger equation in the realistic range of $\bar{A}$. Then, as shown in Appendix, $|\psi(t)\rangle$ can be written as

$$|\psi(t)\rangle = \exp[-i\int_0^t d\tau E_0(\tau)]|\phi_0(t)\rangle + |\delta\psi(t)\rangle. \tag{10}$$

Here, $|\phi_0(t)\rangle$ and $E_0(t)$ are the ground state and the ground state energy of $H(t)$, respectively, and $|\delta\psi(t)\rangle$ is the first order term of the small parameter ϵ of the adiabatic approximation, which is explicitly given in Appendix.

The electronic polarization variation induced by the THz pulse $\Delta P_{\rm el}(t)$ is given by the time integration of current flow as

$$\Delta P_{\rm el}(t) = a\int_{-\infty}^t d\tau\{i_1(\tau) + i_2(\tau)\}. \tag{11}$$

The charge transfer variation $\Delta\rho(t)$ and $\Delta P_{\rm el}(t)$ are given from expectation values $\rho^\sigma_{n,n}(t) = \langle\psi(t)|\hat{\rho}^\sigma_{n,n}|\psi(t)\rangle$ and $i_n(t) = \langle\psi(t)|\hat{i}_n(t)|\psi(t)\rangle$, respectively. The expectation value, for example, $\langle\psi(t)|\hat{\rho}^\sigma_{n,n}|\psi(t)\rangle$ is decomposed into the zeroth order term $\langle\phi_0(t)|\hat{\rho}^\sigma_{n,n}|\phi_0(t)\rangle$ and the terms more than or equal to the first order of ϵ. As shown in Appendix, $\langle\phi_0(t)|\hat{\rho}^\sigma_{n,n}|\phi_0(t)\rangle$ and also the zeroth order term $\langle\phi_0(t)|\hat{i}_n(t)|\phi_0(t)\rangle$ of $i_n(t)$ do not depend on $\bar{A}(t)$ in the infinite system. However, they change with $\bar{A}(t)$ in the finite system, and time variation of the zeroth order term in $\Delta\rho(t)$ and $\Delta P_{\rm el}(t)$ are artifacts caused by the finite-size effect. Because $\Delta\rho(t)$ and $\Delta P_{\rm el}(t)$ are quantities more than or equal to the first order of the small parameter ϵ within the thermodynamic limit, they are seriously affected by this finite-size effect in the zeroth order term. The artifacts can be removed using Eqs. (37) and (39) shown in Appendix, and we consider the charge transfer variation $\Delta\rho(t)$ and electronic polarization variation $\Delta P_{\rm el}(t)$ from which the zeroth order term is removed in the following. We have numerically confirmed these equations by comparing the quantities calculated with $r = 2$ and 3. The difference in $\Delta P_{\rm el}(t)$ is less than 1% for $-5 \le \bar{A} \le 4$, while that in $\Delta\rho(t)$ is less than 1% for $-3 \le \bar{A} \le 3$, and only a few percent for $\bar{A} = -5$, -4, and 4.

We show the time variation of $\Delta\rho(t)$ and $\Delta P_{\rm el}(t)$ for $-4 \le \bar{A} \le 5$ in Fig. 3 (a) and (b), respectively. When $\bar{A} > 0$ ($\bar{A} < 0$) holds and the electric field is in the same (opposite)

direction as the electronic polarization of the ground state, $|P_{\rm el}(t)| > |\bar{P}_{\rm el}|$ ($|P_{\rm el}(t)| < |\bar{P}_{\rm el}|$) and $\rho(t) > \bar{\rho}$ ($\rho(t) < \bar{\rho}$) hold, which is consistent with experiments.[39]

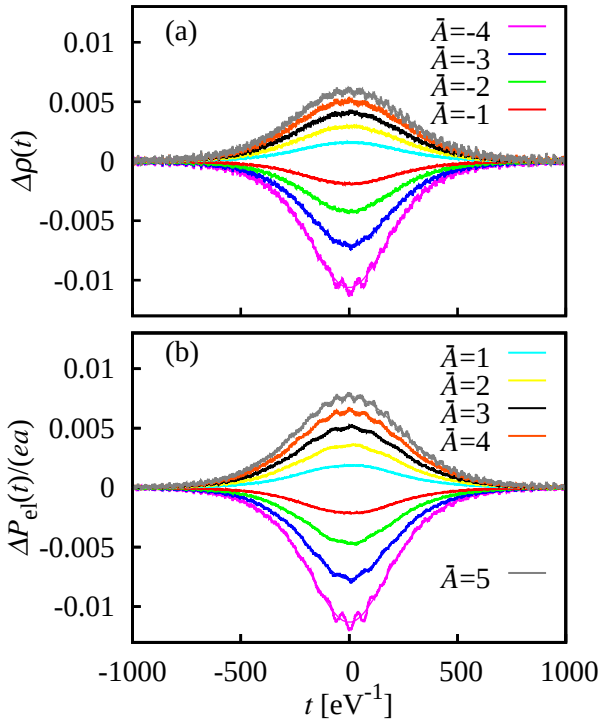

FIG. 3: (Color online) (a) $\Delta\rho(t)$ and (b) $\Delta P_{\rm el}(t)$ for $\bar{A}$=-4, -3, -2, -1, 1, 2, 3, 4, and 5 in the ionic phase (for $\alpha' = 0.13$ and $\beta' = 0.02$), shown with thick lines. The fitting curves $\Delta\tilde{\rho}(E(t))$ and $\Delta\tilde{P}_{\rm el}(E(t))$ are shown with thin lines.

We have numerically found that $\Delta\rho(t)$ and $\Delta P_{\rm el}(t)$ are given by the power series of $E(t)$ up to the fifth order almost exactly, neglecting the small oscillating components. We consider the power series of E given by the following equations:

$$\Delta\tilde{\rho}(E) = \sum_{n=1}^{5} \rho^{(n)} E^n, \tag{12}$$

$$\Delta\tilde{P}_{\rm el}(E) = \sum_{n=1}^{5} P_{\rm el}^{(n)} E^n, \tag{13}$$

and calculate the five coefficients $\rho^{(n)}$ ($P_{\rm el}^{(n)}$) that best fit $\Delta\rho(t)$ ($\Delta P_{\rm el}(t)$) in the time region shown in this figure. The thin lines in Fig. 3 are the fitting curves $\Delta\tilde{\rho}(E(t))$ and $\Delta\tilde{P}_{\rm el}(E(t))$, which reproduce the numerical results very well throughout the time region and for all $\bar{A}$

except for the small oscillating components. The quantities $\Delta\rho(t)$ and $\Delta P_{\rm el}(t)$ at a certain time are determined only by the electric field $E(t)$ at that time, showing that they respond to the electric field instantaneously.

Figure 4 shows $\Delta\tilde{\rho}(E)$ and $\Delta\tilde{P}_{\rm el}(E)$. Both quantities are almost proportional to E for $|E| \lesssim 50$ kV/cm. If the peak magnitude of the electric field is less than 50 kV/cm (for $\bar{A} \lesssim 1$), a linear relationship between $\Delta\rho(t)$ and $E(t)$, and between $\Delta P_{\rm el}(t)$ and $E(t)$ exists. The present results reproduce the important experimental results well. It has been experimentally estimated that $\Delta\tilde{\rho}(E) = 2.5 \times 10^{-3}$ and $\Delta\tilde{P}_{\rm el}(E)/\bar{P}_{\rm el} = 7.5 \times 10^{-3}$ for $E = -38$ kV/cm.[39] These values are also shown in the figure, and are about two times larger than the numerical results. As shown later, the magnitudes of these quantities strongly depend on α'. This point will be discussed later.

For $|E| \gtrsim 50$ kV/cm, nonlinearity becomes prominent, and $\Delta\tilde{\rho}(E)$ and $\Delta\tilde{P}_{\rm el}(E)$ are convex downward. Even in the nonlinear region, $\Delta\rho(t)$ and $\Delta P_{\rm el}(t)$ respond to $E(t)$ with no delay.

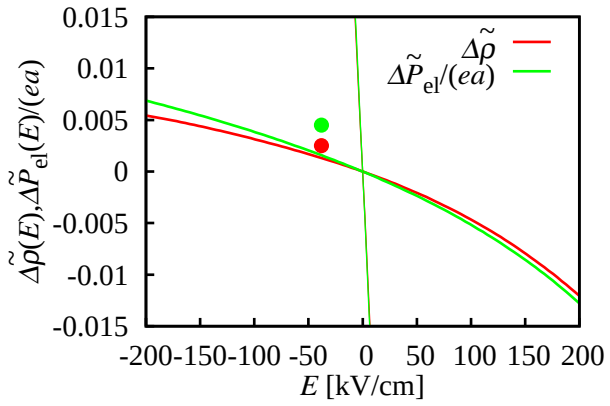

FIG. 4: (Color online) $\Delta\tilde{\rho}(E)$ and $\Delta\tilde{P}_{\rm el}(E)$ for $\alpha' = 0.13$. The experimentally estimated values for $E = -38$ kV/cm are also shown.

As shown in Appendix, a linear relationship exists between $\Delta\rho(t)$ and $\bar{E}(t)$ if the following two conditions are satisfied: (i) the adiabatic approximation holds well ($\epsilon \ll 1$) and (ii) the THz pulse excitation is off-resonant ($\Delta E D \gg 1$), where ΔE is the optical gap. With the present parameters, these conditions hold except for very large $|\bar{A}|$ as discussed below. Consequently, the characteristic instantaneous response of TTF-CA to a THz pulse originates from these two properties.

C. THz pulse induced dynamics in the neutral phase

In this section we show the time variation of $\Delta\rho(t)$ and $\Delta P_{\rm el}(t)$ induced in the neutral phase of TTF-CA by a THz pulse. We calculate $\Delta\rho(t)$ and $\Delta P_{\rm el}(t)$ using Eqs. (38) and (39), respectively, and those for $1 \leq \bar{A} \leq 4$ are shown in Fig. 5. Because $\Delta\rho(t)$ ($\Delta P_{\rm el}(t)$) is an even (odd) function of $\bar{A}$, we show the results for $\bar{A} \geq 0$. The difference in $\Delta\rho(t)$ between the cases of $r = 2$ and 3 is a few percent for $\bar{A} = \pm 4$. Those for $|\bar{A}| \leq 3$, and the difference in $\Delta P_{\rm el}(t)$ for $|\bar{A}| \leq 5$, are less than 1%.

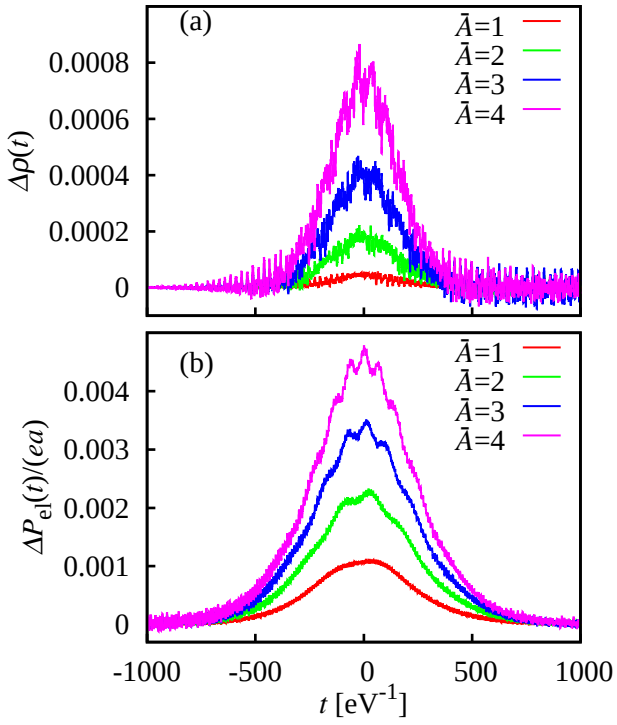

FIG. 5: (Color online) (a) $\Delta\rho(t)$ and (b) $\Delta P_{\rm el}(t)$ for $\bar{A} = 1$, 2, 3, and 4 in the neutral phase (for $\alpha' = 0.158$ and $\beta' = 0$).

As seen from Fig. 5, in spite of the fact that $|\Delta P_{\rm el}(t)|$ are comparable between the neutral and ionic phases, $|\Delta\rho(t)|$ is much smaller in the neutral phase than in the ionic phase at the same value of $\bar{A}$. The important experimental observations[39] are reproduced well by this result.

To consider the origin of the small $\Delta\rho(t)$ in the neutral phase, we investigate the β' dependence of the dynamics, where β' represents the magnitude of bond length alternation. We fix all the parameters except for β', and calculate the dynamics induced by THz pulse

excitation in the range $0 \leq \beta' \leq 0.02$ for $\alpha' = 0.13$ and 0.158. The charge transfer $\bar{\rho}$ for the ground state weakly depends on β', and $\bar{\rho} \simeq 1$ ($\bar{\rho} \simeq 0.1$) holds. Therefore, the ground state stays in the ionic (neutral) state all through the range of β' for $\alpha' = 0.13$ ($\alpha' = 0.158$).

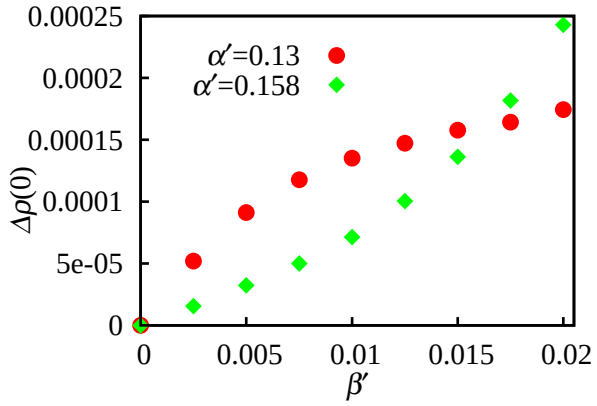

FIG. 6: (Color online) The β' dependence of $\Delta\rho(0)$ for $\bar{A} = 0.1$ in the ionic ($\alpha' = 0.13$) and neutral ($\alpha' = 0.158$) states of TTF-CA.

We show the β' dependence of the peak value of the charge transfer variation $\Delta\rho(0)$ in the ionic ($\alpha' = 0.13$) and neutral ($\alpha' = 0.158$) states in Fig. 6. As seen from this figure, $\Delta\rho(0) \simeq 0$ holds for $\beta' = 0$ both in the ionic and neutral states. This result is analytically shown in Appendix. Namely, $\Delta\rho(t) = 0$ holds up to the first order of the adiabatic parameter ϵ if $\beta' = 0$ holds. The peak value $\Delta\rho(0)$ increases with β' both in the two states, and $|\Delta\rho(t)|$ in the neutral state is comparable to that in the ionic phase at the same value of β'. The much smaller $|\Delta\rho(t)|$ for the neutral phase can be attributed to its inversion symmetry without lattice dimerization.

This can be understood from the balance of the currents between the odd–numbered and the even–numbered bonds. As shown in Eq. (11), $\Delta P_{\rm el}(t)$ is given by the sum of the time integrations of the current at the odd–numbered and even–numbered bonds. Conversely, from the equation of charge conservation (6), $\Delta\rho(t)$ is given by the difference between them as

$$\Delta\rho(t) = \frac{1}{e}\int_{-\infty}^{t} d\tau\{i_2(\tau) - i_1(\tau)\}. \tag{14}$$

Because $|\Delta P_{\rm el}(t)|$ for the neutral phase is comparable to that for the ionic phase, the magnitudes of the time integrations of current at each bond are also comparable for the two

phases. In the case of uniform lattice ($\beta' = 0$), $i_{2n-1}(\tau) \simeq i_{2n}(\tau)$ holds and the current at the odd–numbered bonds nearly cancels out that at the even–numbered bonds. This is the reason for the very small $\Delta\rho(t)$ in the neutral phase.

D. Phase boundary region

In this section we show the dynamics induced by a THz pulse in the phase boundary region. We adopt the parameters $\alpha' = 0.1445$ and $\beta' = 0.02$ ($\alpha' = 0.142$ and $\beta' = 0$), which reproduce the experimentally obtained charge transfer 0.6 (0.3)[27,28] for the ionic (neutral) phase. With these parameters, $\bar{\rho} = 0.62$ ($\bar{\rho} = 0.32$) holds in the ionic (neutral) phase, and $\alpha' = 0.1445$ and $\alpha' = 0.142$ are in the phase boundary region, where $\bar{\rho}$ decreases rapidly as α' increases as seen in Fig. 2.

We first discuss the results for the ionic phase. The differences between the values of $\Delta\rho(t)$ and $\Delta P_{\rm el}(t)$ calculated with $r = 2$ and 3 are both less than 1% for $-1 \leq \bar{A} \leq 1$. Thus, the time variation of $\Delta\rho(t)$ and $\Delta P_{\rm el}(t)$ for $-1 \leq \bar{A} \leq 1$ are shown in Fig. 7 (a) and (b), respectively.

Also in the phase boundary region, $\Delta\rho(t)$ and $\Delta P_{\rm el}(t)$ are approximated well by the power series of $E(t)$ up to the fifth order. The fitting curves $\Delta\tilde{\rho}(E(t))$ and $\Delta\tilde{P}_{\rm el}(E(t))$ are also shown in Fig. 7 (a) and (b), respectively. The fitting curves agree well with $\Delta\rho(t)$ and $\Delta P_{\rm el}(t)$, and the linear relationship between $\Delta\rho(t)$ and $E(t)$, and between $\Delta P_{\rm el}(t)$ and $E(t)$ hold well for $|\bar{A}(t)| \lesssim 0.2$ ($|E(t)| \lesssim 10$ kV/cm). The deviations from the fitting curves become prominent for $|\bar{A}(t)| \gtrsim 0.2$. However, the overall time profiles of $\Delta\rho(t)$ and $\Delta P_{\rm el}(t)$ are reproduced well by $\Delta\tilde{\rho}(E(t))$ and $\Delta\tilde{P}_{\rm el}(E(t))$, respectively, and nearly instantaneous response also occurs in the phase boundary region.

Figure 4 also shows $\Delta\tilde{\rho}(E)$ and $\Delta\tilde{P}_{\rm el}(E)$ for the ionic phase in the phase boundary region. As seen, $\Delta\tilde{\rho}(E)$ and $\Delta\tilde{P}_{\rm el}(E)$ for $\alpha' = 0.1445$ are about 50 times larger than those for $\alpha' = 0.13$. The charge and polarization respond to the electric field much more sensitively inside the phase boundary region than outside the region. Furthermore, the magnitude of the charge transfer $|\Delta\rho(t)|$ is much smaller in the neutral phase than in the ionic phase.

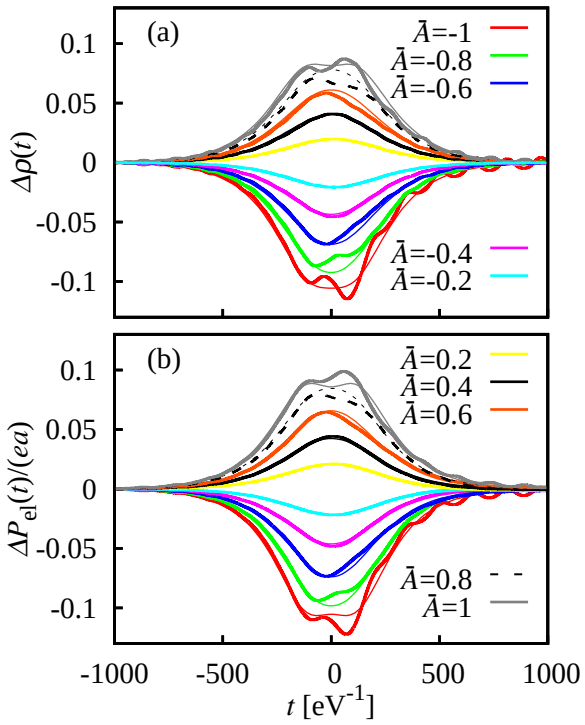

FIG. 7: (Color online) (a) $\Delta\rho(t)$ and (b) $\Delta P_{\rm el}(t)$ for $\bar{A}$=-1, -0.8, -0.6, -0.4, -0.2, 0.2, 0.4, 0.8, and 1 in the ionic phase in the phase boundary region (for $\alpha' = 0.1445$ and $\beta' = 0.02$), shown by the thick lines. The fitting curves $\Delta\tilde{\rho}(E(t))$ and $\Delta\tilde{P}_{\rm el}(E(t))$ are represented by the thin lines.

IV. DISCUSSION

It has been experimentally shown that there is an approximate linear relationship between $\Delta\rho(t)$ and $E(t)$, and $|\Delta\rho(t)|$ is much larger in the ionic phase than in the neutral phase.[39] These results are reproduced well by our numerical calculations. As shown in the previous section, this characteristic charge dynamics occurs if the following two conditions are satisfied: (i) the adiabatic approximation holds well ($\epsilon = \max(|J_{n,0}|/(\omega_n)^2)\bar{A}/D \ll 1$) and (ii) the THz pulse excitation is off-resonant ($\Delta E D \gg 1$). For $\alpha' = 0.13$ and $\beta' = 0.02$, $\max(|J_{n,0}|/\omega_n^2) \simeq 0.6$ and $\Delta E \simeq 0.5$ hold. Therefore, these characteristic instantaneous charge dynamics induced by the THz pulse excitation occur even at five times smaller D for the realistic magnitude $\bar{A} \lesssim 1$. We have confirmed this with numerical calculations. It is therefore expected that the polarization amplitude in ionic phase TTF-CA can be modulated on a 0.1 picosecond time scale by a THz pulse.

Large optical gap is an indispensable property for materials in which this characteristic

instantaneous response occurs. However, charge susceptibility is very small and $|\Delta\rho(t)|$ and $|\Delta P_{\rm el}(t)|$ are considered to be very small in conventional insulators. Significant and instantaneous changes in charge and polarization with $E(t)$ are characteristic of materials with large optical gap and large charge susceptibility. In the case of TTF-CA, its characteristic large valence fluctuation enables their coexistence.

Because the adiabatic approximation holds well, heat production is negligible for realistic magnitudes of the THz pulse field. This is a big merit for optical devices. However, neither polarization reversal in the ionic phase nor THz pulse induced transition between the neutral and ionic phases occurs within the adiabatic picture. They have not been observed also experimentally.[39] As seen from Eq. (30), the induced charge arises from the off-diagonal element between the adiabatic ground state and virtual excited states. This is in contrast to the case of photoexcitation, where real excitation plays an important role and photoinduced phase transition between the neutral and ionic phases occurs.[43,44,57–65] However, by using a stronger THz pulse to the TTF-CA very close to the phase boundary, polarization reversal or the phase transition may be induced by a THz pulse. To address this problem, the following points are to be considered. It is difficult to remove artifacts caused by the finite-size effect in the intense excitation case. We need to extend the present method to describe the dynamics in the case. Furthermore, the screening of Coulomb interaction is enhanced near the phase boundary by the diverging dielectric constant,[32,49] which may seriously affect the phase transition or polarization reversal. However, the electronic parameters are fixed, and this screening effect cannot be described in the present extended Hubbard model. We consider that electron-lattice coupling may play a crucial role to realize these phenomena. By introducing electron-lattice coupling in the transfer integral, THz pulse excitation may induce the lattice motion that reverses the phase of bond length alternation, which will induced the electronic polarization reversal. These points will be discussed in a forthcoming paper.

V. CONCLUSION

We have investigated the dielectric properties of TTF-CA using exact numerical calculations of an extended Hubbard model. The electronic polarization $\bar{P}_{\rm el}$ of the ionic ground state is obtained by directly calculating the adiabatic flow of current. The direction of $\bar{P}_{\rm el}$

is opposite to that of the polarization $\bar{P}_{\rm ion}$ owing to ionic displacement, and $|\bar{P}_{\rm el}|$ is much larger than $|\bar{P}_{\rm ion}|$, showing that in the ionic phase, TTF-CA is an electric ferroelectric. These results are consistent with experiments and previous theoretical results based on density functional theory. Furthermore, we numerically calculated the dynamics induced by THz pulse excitation. The major experimental results are reproduced well by our numerical results. For the ionic phase, there exists almost exact linear relationship between the charge transfer variation induced by the THz pulse $\Delta\rho(t)$ and the electric field $E(t)$ of the pulse, and between the electric polarization variation induced by the THz pulse $\Delta P_{\rm el}(t)$ and $E(t)$ in the realistic range of excitation magnitude. The absolute value of $\Delta\rho(t)$ for the neutral phase is much smaller than that for the ionic phase. These properties are found to originate from the adiabatic nature of the THz pulse excited state.

VI. ACKNOWLEDGEMENTS

This work was supported by JSPS KAKENHI Grant Number JP16K05402, and CREST, JST.

VII. APPENDIX

In this appendix, we derive the condition under which the characteristic instantaneous charge dynamics occurs, and how artifacts caused by the finite-size effect are romoved. Up to the first order of the small parameter ϵ of the adiabatic approximation, which will be described later, the solution $|\psi(t)\rangle$ of the time-dependent Schrödinger equation can be written as

$$|\psi(t)\rangle = \exp[-i\int_0^t d\tau E_0(\tau)]|\phi_0(t)\rangle + |\delta\psi(t)\rangle, \tag{15}$$

$$|\delta\psi(t)\rangle = \sum_n^{n\neq 0} c_n(t)\exp[-i\int_0^t d\tau E_n(\tau)]|\phi_n(t)\rangle, \tag{16}$$

where $|\phi_n(t)\rangle$ is the energy eigenstate of $H(t)$ with an energy eigen value $E_n(t)$, and $|\phi_0(t)\rangle$ and $E_0(t)$ are the ground state and the ground state energy, respectively. Note that the magnitude of the coefficient for $|\phi_0(t)\rangle$ is equal to 1 up to the first order. The first order term $|\delta\psi(t)\rangle$ is given by the linear combination of $|\phi_n(t)\rangle$ with the coefficient $c_n(t)$.

To derive differential equation for $c_n(t)$, we consider the terms up to the first order of infinitesimal time change Δt in the following. We divide the Hamiltonian $H(t+\Delta t)$ into the unperturbed part $H_0 = H(t)$ and perturbed part $H_1 = H(t+\Delta t) - H(t)$. Up to the first order of Δt, H_1 can be written as

$$H_1 = \hat{J}(t)\bar{E}(t)\Delta t, \tag{17}$$

where $\hat{J}(t)$ is given by

$$\hat{J}(t) = \frac{1}{e}\sum_{n=1}^{N} \hat{i}_n, \tag{18}$$

and $\bar{E}(t)$ is given by

$$\bar{E}(t) = -\frac{d}{dt}\bar{A}(t) = eaE(t). \tag{19}$$

From the stationary perturbation theory, $|\phi_k(t+\Delta t)\rangle$ is given by

$$|\phi_k(t+\Delta t)\rangle = |\phi_k(t)\rangle - \bar{E}(t)\Delta t \sum_{n}^{n\neq k} \frac{J_{n,k}(t)}{E_n(t) - E_k(t)}|\phi_n(t)\rangle, \tag{20}$$

where $J_{n,k}(t)$ is the transition dipole moment given by

$$J_{n,k}(t) = \langle\phi_n(t)|\hat{J}(t)|\phi_k(t)\rangle. \tag{21}$$

The arbitrary phase of $|\phi_k(t+\Delta t)\rangle$ is determined from this equation.

From the time-dependent perturbation theory, $|\psi(t+\Delta t)\rangle$ is obtained up to the first order of $\bar{A}$ as,

$$\begin{aligned} |\psi(t+\Delta t)\rangle \;&=\; U^{(0)}(t+\Delta t,t)\exp[-i\int_0^t d\tau E_0(\tau)]|\phi_0(t)\rangle \\ &+\; U^{(1)}(t+\Delta t,t)\exp[-i\int_0^t d\tau E_0(\tau)]|\phi_0(t)\rangle + U^{(0)}(t+\Delta t,t)|\delta\psi(t)\rangle, \end{aligned} \tag{22}$$

where $U^{(i)}(t+\Delta t,t)$ is the ith order time evolution operator given by

$$U^{(0)}(t+\Delta t,t) \;=\; \exp[-iH(t)\Delta t], \tag{23}$$

$$U^{(1)}(t+\Delta t,t) \;=\; -i\int_0^{\Delta t} d\tau U^{(0)}(t+\Delta t,t+\tau)\hat{J}(t)\bar{E}(t)\tau U^{(0)}(t+\tau,t). \tag{24}$$

Substituting Eqs. (23) and (24) into Eq. (22), we obtain

$$\begin{aligned} |\delta\psi(t+\Delta t)\rangle \;&=\; \sum_{n}^{n\neq 0}\{c_n(t)\exp[-i\int_0^t d\tau E_n(\tau)] \\ &+\; i\bar{E}(t)\exp[-i\int_0^t d\tau E_0(\tau)](\frac{1}{E_n(t)-E_0(t)})^2 J_{n,0}(t)\} \\ &\times\; \{\exp(-iE_n(t)\Delta t) - \exp(-iE_0(t)\Delta t)\}|\phi_n(t)\rangle, \end{aligned} \tag{25}$$

From Eq. (25), it can be easily shown that $c_n(t)$ satisfies the following differential equation:

$$\frac{d}{dt}c_n(t) = \exp[i\int_0^t d\tau\omega_n(\tau)]\bar{E}(t)\frac{J_{n,0}(t)}{\omega_n(t)}, \tag{26}$$

where $\omega_n(t) = E_n(t) - E_0(t)$ is the excitation energy from the ground state to the optically allowed energy eigenstate $|\phi_n(t)\rangle$, where $J_{n,0}(t) \neq 0$ holds. As shown later, in the thermodynamic limit, $J_{n,0}(t)$ and $\omega_n(t)$ are constant with time, and $J_{n,0}(t) = J_{n,0}$ and $\omega_n(t) = \omega_n$ hold, where $J_{n,0}$ and ω_n are the transition dipole moment and the excitation energy, respectively, from $|\phi_0\rangle$ to $|\phi_n\rangle$ in the electronic Hamiltonian $H_{\rm e} = H(-\infty)$. Then, we can solve the differential equation (26), and $c_n(t)$ is given by

$$c_n(t) = -i\frac{J_{n,0}}{\omega_n^2}\exp[i\omega_n t]\bar{E}(t) = -i\frac{J_{n,0}\bar{A}}{2\omega_n^2 D}\exp[i\omega_n t]\mathrm{sech}^2(\frac{t}{D}), \tag{27}$$

where the terms of second order or more in $1/(\omega_n D)$ are neglected. In the case of THz pulse excitation, $1/(\Delta E D) \ll 1$ holds, and this approximation holds well for almost all the insulators. Therefore, the small parameter ϵ for the adiabatic approximation is given by

$$\epsilon = \max(\frac{|J_{n,0}|}{\omega_n^2})\frac{|\bar{A}|}{D}, \tag{28}$$

and the adiabatic approximation is good if $\epsilon \ll 1$ holds.

We expand $\rho(t) = \langle\psi(t)|\sum_\sigma \hat{\rho}^\sigma_{2,2}|\psi(t)\rangle$ up to the first order of ϵ as $\rho(t) = \rho^{(0)}(t) + \rho^{(1)}(t)$, where $\rho^{(i)}(t)$ is the ith order term. From Eq. (15), it can be easily shown that

$$\rho^{(0)}(t) \;=\; \langle\phi_0(t)|\sum_\sigma \hat{\rho}^\sigma_{2,2}|\phi_0(t)\rangle, \tag{29}$$

$$\rho^{(1)}(t) \;=\; 2\mathrm{Re}[\exp[i\int_0^t d\tau E_0(\tau)]\langle\phi_0(t)|\sum_\sigma \hat{\rho}^\sigma_{2,2}|\delta\psi(t)\rangle]. \tag{30}$$

The zeroth order term does not depend on time and $\rho^{(0)}(t) = \bar{\rho}$ holds in the thermodynamic limit as shown below. Using the unitary transformation

$$\tilde{c}_{n,\sigma} = c_{n,\sigma}\exp[in\bar{A}(t)], \tag{31}$$

where $\tilde{c}^\dagger_{n,\sigma}\tilde{c}_{n,\sigma} = c^\dagger_{n,\sigma}c_{n,\sigma}$ holds, the transfer term of $H(t)$ can be written as

$$\begin{aligned}&\sum_{n=1,\sigma}^{N-1}(\bar{\beta} + \beta'(-1)^n)(\tilde{c}^\dagger_{n,\sigma}\tilde{c}_{n+1,\sigma} + \tilde{c}^\dagger_{n+1,\sigma}\tilde{c}_{n,\sigma})\\ +\;&(\bar{\beta} + \beta'(-1)^N)(\tilde{c}^\dagger_{N,\sigma}\tilde{c}_{1,\sigma}\exp[iN\bar{A}(t)] + \tilde{c}^\dagger_{1,\sigma}\tilde{c}_{N,\sigma}\exp[-iN\bar{A}(t)]).\end{aligned} \tag{32}$$

The vector potential gives a twist in the boundary condition, but does not change $H(t)$ except for this. This holds also for $\hat{J}(t)$. Therefore, $\langle\phi_n(t)|\sum_\sigma \hat{\rho}^\sigma_{2,2}|\phi_m(t)\rangle - \langle\phi_n|\sum_\sigma \hat{\rho}^\sigma_{2,2}|\phi_m\rangle$, $J_{n,0}(t) - J_{n,0}$, and $\omega_n(t) - \omega_n$ are of the order of $1/N$ at most.

Substituting Eq. (27) into Eq. (30), and neglecting the finite-size effect of the order of $1/N$, we obtain $\Delta\rho(t)$ as

$$\Delta\rho(t) = G\bar{E}(t), \tag{33}$$

$$G = 2\mathrm{Im}[\sum_n^{n\neq 0} \frac{J_{n,0}}{\omega_n^2}\langle\phi_0|\sum_\sigma \hat{\rho}^\sigma_{2,2}|\phi_n\rangle] = 2\mathrm{Im}[\langle\phi_0|\sum_\sigma \hat{\rho}^\sigma_{2,2}\frac{1}{\{H_\mathrm{e}-E_0\}^2}\hat{J}|\phi_0\rangle], \tag{34}$$

up to the first order of ϵ, where $\hat{J} = \hat{J}(-\infty)$. The quantity G is constant with time in the thermodynamic limit.

Up to the first order of ϵ, $|\psi(t)\rangle$ is given by the linear combination of $|\phi_0(t)\rangle$ and $|\phi_n(t)\rangle$ where $J_{n,0} \neq 0$ holds, as seen from Eqs. (15), (16) and (27). As a result, $\Delta\rho(t)$ is given from off-diagonal elements $\langle\phi_0|\sum_\sigma \hat{\rho}^\sigma_{2,2}|\phi_n\rangle$ as shown in Eq. (34). In the uniform lattice ($\beta' = 0$), H_e and $\sum_\sigma \hat{\rho}^\sigma_{2,2}$ are symmetric, and $\hat{J}$ is antisymmetric with respect to site 2. Because of the symmetry, the ground state $|\phi_0\rangle$ is symmetric, and $|\phi_n\rangle$ are all antisymmetric, which results in $\langle\phi_0|\sum_\sigma \hat{\rho}^\sigma_{2,2}|\phi_n\rangle = 0$. Therefore, $G = 0$ holds for the uniform lattice.

If we consider the higher order terms, namely, excitation from the weakly excited state, the elements between symmetric states and those between antisymmetric states contribute to $\Delta\rho(t)$, and $\Delta\rho(t)$ becomes nonzero even for $\beta' = 0$. We have confirmed this from the numerical calculation. There is no linear relation between $\Delta\rho(t)$ and $\bar{E}(t)$ in the case of $\beta' = 0$.

The time variations of the zeroth order terms $\langle\phi_0(t)|\hat{\rho}^\sigma_{n,n}|\phi_0(t)\rangle$ of $\rho^\sigma_{n,n}$ and $\langle\phi_0(t)|\hat{i}_n|\phi_0(t)\rangle$ of $\hat{i}_n$ are artifacts caused by the finite-size effect as shown before. These artifacts can be removed by considering the dynamics induced by a pulse with renormalized duration rD given by

$$\bar{A}^{(r)}(t) = \frac{\bar{A}}{2}\{1 + \tanh(\frac{t}{rD})\}. \tag{35}$$

Because $H^{(r)}(rt) = H(t)$ holds, where $H^{(r)}(t)$ is the Hamiltonian with the pulse described by $\bar{A}^{(r)}(t)$, the time-dependent solution $|\psi^{(r)}(t)\rangle$ of $H^{(r)}(t)$ can be written as

$$|\psi^{(r)}(rt)\rangle = \exp[-ir\int_0^t d\tau E_0(\tau)]|\phi_0(t)\rangle + |\delta\psi^{(r)}(rt)\rangle, \tag{36}$$

where $|\delta\psi^{(r)}(t)\rangle$ is the first order term of ϵ/r. The zeroth order term can be removed using Eqs. (15) and (36), and $\Delta\rho(t)$ in the ionic phase is given by

$$\Delta\rho(t) = \frac{r}{r-1}\{\langle\psi(t)|\hat{\rho}_{2,2}|\psi(t)\rangle - \langle\psi^{(r)}(rt)|\hat{\rho}_{2,2}|\psi^{(r)}(rt)\rangle\}, \tag{37}$$

$\Delta\rho(t)$ in the neutral phase is given by

$$\Delta\rho(t) = \frac{r^2}{r^2-1}\{\langle\psi(t)|\hat{\rho}_{2,2}|\psi(t)\rangle - \langle\psi^{(r)}(rt)|\hat{\rho}_{2,2}|\psi^{(r)}(rt)\rangle\}, \tag{38}$$

and $\Delta P_{\rm el}(t)$ in both the two phases is given by

$$\Delta P_{\rm el}(t) = \frac{ar^2}{r^2-1}\int_{-\infty}^{t} d\tau\{\langle\psi(\tau)|(\hat{i}_1(\tau)+\hat{i}_2(\tau))|\psi(\tau)\rangle - \langle\psi^{(r)}(r\tau)|(\hat{i}_1(\tau)+\hat{i}_2(\tau))|\psi^{(r)}(r\tau)\rangle\}, \tag{39}$$

where we use the fact that the leading term of $\langle\psi^{(r)}(rt)|\hat{\rho}_{2n,2n}|\psi^{(r)}(rt)\rangle - \langle\phi_0(t)|\hat{\rho}_{2n,2n}|\phi_0(t)\rangle$ is the first (second) order of ϵ/r in the ionic (neutral) phase, and that of $\langle\psi^{(r)}(r\tau)|\hat{i}_n|\psi^{(r)}(r\tau)\rangle - \langle\phi_0(t)|\hat{i}_n|\phi_0(t)\rangle$ is the second order of ϵ/r in both the two phases.

---

[1] K. Uchino, Ferroelectric Devices (Marcel Dekker, New York 2000).

[2] M. E. Lines and A. M. Glass, Principles and Applications of Ferroelectrics and Related Materials (Oxford University, New York 1977).

[3] J. F. Scott, Science **315**, 954 (2007).

[4] J. van den Brink and D. I. Khomskii, J. Phys. Condens. Matter **20**, 434217 (2008).

[5] S. Ishihara, J. Phys. Soc. Jpn. **79**, 011010 (2010).

[6] T. Kimura, T. Goto, H. Shintani, K. Ishizaka, T. Arima, and Y. Tokura, Nature **426**, 55 (2003).

[7] J. Wang, J. B. Neaton, H. Zheng, V. Nagarajan, S. B. Ogale, B. Liu, D. Viehland, V. Vaithyanathan, D. G. Schlom, U. V. Waghmare, N. A. Spaldin, K. M. Rabe, M. Wuttig, and R. Ramesh, Science **299**, 1719 (2003).

[8] N. A. Spaldin and M. Fiebig, Science **309**, 391 (2005).

[9] W. Eerenstein, N. D. Mathur and J. F. Scott, Nature (London) **442**, 759 (2006).

[10] S.-W Cheong and M. Mostovoy, Nature Mater. **6**, 13@(2007).

[11] S. Picozzi, K. Yamauchi, B. Sanyal, I. A. Sergienko, and E. Dagotto, Phys. Rev. Lett. **99**, 227201 (2007).

[12] P. Lunkenheimer, J. Müller, S. Krohns, F. Schrettle, A. Loidl, B. Hartmann, R. Rommel, M. de Souza, C. Hotta, J. A. Schlueter, and M. Lang, Nature Materials **11**, 755 (2012).

[13] N. Ikeda, H. Ohsumi, K. Ohwada, K. Ishii, T. Inami, K. Kakurai, Y. Murakami, K. Yoshii, S. Mori, Y. Horibe, and H. Kito, Nature **436**, 1136 (2005).

[14] A. Nagano, M. Naka, J. Nasu, and S. Ishihara, Phys. Rev. Lett. **99**, 217202 (2007).

[15] M. Naka, A. Nagano, and S. Ishihara, Phys. Rev. B **77**, 224441 (2008).

[16] P. Monceau, F. Ya. Nad, and S. Brazovskii, Phys. Rev. Lett. **86**, 4080 (2001).

[17] H. Yoshioka, M. Tsuchiizu, and H. Seo, J. Phys. Soc. Jpn. **76**, 103701 (2007).

[18] Y. Otsuka, H. Seo, Y. Motome, and T. Kato, J. Phys. Soc. Jpn. **77**, 113705 (2008).

[19] K. Yamamoto, S. Iwai, S. Boyko, A. Kashiwazaki, F. Hiramatsu, C. Okabe, N. Nishi, and K. Yakushi, J. Phys. Soc. Jpn. **77**, 074709 (2008).

[20] J. B. Torrance, J. E. Vazquez, J. J. Mayerle, and V.Y. Lee, Phys. Rev. Lett. 46, 253 (1981).

[21] H. M. McConnell, B. M. Hoffman, and R. M. Metzger, Proc. Natl. Acad. Sci. U.S.A. **53**, 46 (1965).

[22] J. B. Torrance, A. Girlando, J. J. Mayerle, J. I. Crowley, V. Y. Lee, P. Batail, and S. J. LaPlaca, Phys. Rev. Lett. **47**, 1747 (1981).

[23] M. H. Lemée-Cailleau, M. Le Cointe, H. Cailleau, T. Luty, F. Moussa, J. Roos, D. Brinkmann, B. Toudic, C. Ayache, and N. Karl, Rev. Lett. **79**, 1690 (1997)

[24] A. Girlando, A. Painelli, S. Bewick, and Z. Soos, Synth. Met. **141**, 129 (2004).

[25] M. Masino, A. Girlando, A. Brillante, R.G. Della Valle, E. Venuti, N. Drichko, and M. Dressel, Chem. Phys. **325**, 71 (2006)

[26] G. DAvino and M. J. Verstraete, Phys. Rev. Lett. **113**, 237602 (2014)

[27] A. Girlando, F. Marzola, C. Pecile, and J. B. Torrance, J. Chem. Phys. **79**, 1075 (1983).

[28] S. Horiuchi, Y. Okimoto, R. Kumai, and Y. Tokura, J. Phys. Soc. Jpn. **69**, 1302 (2000).

[29] M. Le Cointe, M. H. Lemee-Cailleau, H. Cailleau, B. Toudic, L. Toupet, G. Heger, F. Moussa, P. Schweiss, K. H. Kraft, and N. Karl, Phys. Rev. **B 51**, 3374 (1995).

[30] Y. Tokura, S. Koshihara, Y. Iwasa, H. Okamoto, T. Komatsu, T. Koda, N. Iwasawa, and G. Saito, Phys. Rev. Lett. **63**, 2405 (1989).

[31] P. Garcia, S. Dahaoui, C. Katan, M. Souhassou, and C. Lecomte, Faraday Discuss. **135**, 217 (2007).

[32] H. Okamoto, T. Mitani, Y. Tokura, S. Koshihara, T. Komatsu, Y. Iwasa, T. Koda, and G. Saito, Phys. Rev. **B 43**, 8224 (1991).

[33] H. Kishida, H. Takamatsu, K. Fujinuma, and H. Okamoto, Phys. Rev. **B 80**, 205201 (2009).

[34] K. Kobayashi, S. Horiuchi, R. Kumai, F. Kagawa, Y. Murakami, and Y. Tokura, Phys. Rev. Lett. **108**, 237601 (2012).

[35] G. Giovannetti, S. Kumar, A. Stroppa, J. van den Brink, and S. Picozzi, Phys. Rev. Lett. **103**, 266401 (2009).

[36] S. Ishibashi and K. Terakura, Physica B (Amsterdam) **405**, S338 (2010).

[37] S. Ishibashi and K. Terakura, J. Phys. Soc. Jpn. **83** 073702 (2014).

[38] K. Terakura and S. Ishibashi, Phys. Rev. **B 91** 195120 (2015).

[39] T. Miyamoto, H. Yada, H. Yamakawa, and H.i Okamoto, Nat. Commun. 4:2586 doi: 10.1038/ncomms3586 (2013).

[40] N. Tsuji, T. Oka, H. Aoki, and P. Werner, Phys. Rev. **B 85**, 155124 (2012).

[41] T. Oka, Phys. Rev. **B 86**, 075148 (2012).

[42] E. G. Lewars, Computational Chemistry: Introduction to the Theory and Applications of Molecular and Quantum Mechanics (Springer 2016).

[43] K. Iwano, Phys. Rev. Lett. **97**, 226404 (2006).

[44] K. Yonemitsu, J. Phys. Soc. Jpn. **80**, 084707 (2011).

[45] N. Nagaosa and J. Takimoto, J. Phys. Soc. Jpn. **55**, 2735 (1986).

[46] A. Painelli and A. Girlando, Phys. Rev. **B 37**, 5748 (1988).

[47] L. Del Freo, A. Painelli, and Z. G. Soos, Phys. Rev. Lett. **89**, 027402 (2002).

[48] M. Tsuchiizu and A. Furusaki, Phys. Rev. **B 69**, 035103 (2004).

[49] Z. G. Soos, S. A. Bewick, A. Peri, and A. Painelli, J. Chem. Phys. **120**, 6712 (2004).

[50] R. D. King-Smith and D. Vanderbilt, Phys. Rev. **B 47**, 1651 (1993).

[51] R. Resta, Rev. Mod. Phys. **66**, 899 (1994).

[52] R. E. Cohen, Nature (London) **358**, 136 (1992).

[53] T. Egami, S. Ishihara, and M. Tachiki, Science **261**, 1307 (1993).

[54] D. Vanderbilt and R. D. King-Smith, Phys. Rev. **B 48**, 4442 (1993).

[55] S. Onoda, S. Murakami, and N. Nagaosa, Phys. Rev. Lett. **93**, 167602 (2004).

[56] R. Nourafkan and G. Kotliar, Phys. Rev. **B 88**, 155121 (2013)

[57] T. Luty, H. Cailleau, S. Koshihara, E. Collet, M. Takesada, M. H. Lemee-Cailleau, M. Buron-Le Cointe, N. Nagaosa, Y. Tokura, E. Zienkiewicz and B. Ouladdiaf, Europhys. Lett. **59**, 619 (2002).

[58] E. Collet, M.-H. Leme-Cailleau, M. Buron-Le Cointe, H. Cailleau, M. Wulff, T. Luty, S.-Y.

Koshihara, M. Meyer, L. Toupet, P. Rabiller, and S. Techert, Science **300**, 612 (2003).

[59] H. Okamoto, Y. Ishige, S. Tanaka, H. Kishida, S. Iwai, and Y. Tokura, Phys. Rev. **B 70**, 165202 (2004).

[60] H. Uemura, H. Okamoto, Phys. Rev. Lett. **105**, 258302 (2010).

[61] T. Miyamoto, K. Kimura, T. Hamamoto, H. Uemura, H. Yada, H. Matsuzaki, S. Horiuchi, and H. Okamoto,Phys. Rev. Lett. **111** 187801 (2013)

[62] K. Iwano, Phys. Rev. Lett. **102** 106405 (2009).

[63] K. Iwano, Phys. Rev. **B 84**, 235139 (2011).

[64] Y. Nakatsuka, T. Tsuneda, T. Sato, and K. Hirao, J. Chem. Theory Comput. **7** 2233 (2011)

[65] L. Cavatorta, A. Painelli, and Z. G. Soos, Phys. Rev. **B 91** 174301 (2015)